
Concurrent EPR and fluorescence studies of the effect of sequences of fluctuating low levels of ozone on Kentucky bluegrass

U. Mazarura*

University of Zimbabwe, Crop Science Department, P. O. Box MP 176 Mt Pleasant, Harare, Zimbabwe

U. Mazarura (2013) Concurrent EPR and fluorescence studies of the effect of sequences of fluctuating low levels of ozone on Kentucky bluegrass. International Journal of Agricultural Technology 9(1):211-226.

Abstract Tropospheric ozone (O_3) is one of the most important air pollutants whose mechanism of action is not very well understood. Hence in an attempt to shed some light to how O_3 affects plants, studies with a C-3 grass, *Poa pratensis* L., Kentucky bluegrass, treated with sine-wave exposures to O_3 within the modified cavity of an electron paramagnetic resonance (EPR) spectrometer, permitting observation of the effects of exposure on both the free radical signals in photosystems I and II and on chlorophyll fluorescence attributable to photosystem II were carried out. Both Signal I (from $P700^+$ in PSI) and Signal II (from Tyr-160 in the D2 protein of PSII) were stimulated by O_3 . However, the fact that Signal I observed in white light in bluegrass during exposure to O_3 rose to the level of Signal I in far-red light, indicated impaired–electron flow through PSI. These effects and concomitant effects on chlorophyll fluorescence confirm a major effect of O_3 on the water-splitting side of PSII. The level of Signal I in white light was approximately one half of that in far-red light.

Key words: signal I, photosystem II, *Poa pratensis*; free radicals; Signal I; C-3

Introduction

Ozone-induced effects on plants range from clear injury symptoms such as chlorosis or necrosis to subtle metabolic changes (Heath, 1988) resulting in reduced photosynthesis leading to reduce growth and yield (Runeckles and Chevone, 1992). Based mainly on theoretical grounds toxic oxyradicals such as superoxide anion and hydroxyl have been implicated in plant response to O_3 exposure because of the possibilities of their formation during reactions of O_3 with cell constituents and their high reactivity and potential for membrane perturbation (Mudd, 1982; Bhalia *et al.*, 2012).

* Corresponding author: U. Mazarura; e-mail: umazarura@agric.uz.ac.zw

Superoxide is produced normally in the photosynthetic electron transport system, but is scavenged by superoxide dismutase (SOD) and other antioxidants such as ascorbic acid, peroxidase, glutathione and α -tocopherol (Asada and Takahashi, 1987) thereby reducing its potential toxicity. Hence superoxide-induced adverse effects are thought to be a result of reduced scavenging, elevated production or both.

Until recently, evidence for the involvement of superoxide in O₃ phytotoxicity has been circumstantial demonstrated and mainly based on observations of the activity of SOD. Increased SOD activity as a result of exposure to O₃ was reported by Lee and Bennett (1982) in bean (*Phaseolus vulgaris*) and Declaire *et al.*, (1984) in spinach (*Spinacia oleracea*) leaves. Reports of decreased SOD levels also exist (*Spinacia oleracea*; Sakaki *et al.*, 1983). Chanway and Runeckles (1984) only detected increased SOD in bean leaves at the onset of necrosis. However, Runeckles and Vaartnou (1997) presented evidence for transient superoxide formation in grass and radish leaves exposed to 100ppb O₃, based on electron paramagnetic resonance (EPR) spectroscopic evidence.

EPR provides a unique means of direct detection and characterization of free radical spectra. Two free radical signals associated with the photosynthetic apparatus can usually be detected in intact leaves *in situ* (Runeckles and Vaartnou, 1992). One, it is relatively stable and persists in darkness (Signal II) and is attributable to tyrosine residues on the D1 and D2 peptides of photosystem II (Barry and Babcock, 1987). A second distinct Signal (I) appears upon illumination with white light, and is usually enhanced in far-red light (>700nm). Signal I is thought to be produced by oxidized chlorophyll P700 in photosystem I (Beinert *et al.*, 1962), and disappears rapidly when illumination ceases. In 710nm illumination, Signal I is indicative of cyclic electron flow in photosystem I.

Chlorophyll fluorescence measurements have been used by several workers studying the effects of O₃ on a range of species following the early report of Schreiber *et al.* (1978). Since then ozone has been reported to cause decreases in maximum chlorophyll fluorescence quantum yield (Fv/Fm), actual quantum yield (Y) and photochemical quenching (qP), and increased non-photochemical quenching (NPQ) (see review by Bussotti *et al.*, 2011; Calatayud, 2007; Calatayud and Barreno. 2004; Calatayud *et al.*, 2006). Since changes in such fluorescence are attributable to changes in photosystem II, the combination of EPR and fluorescence measurements permits the simultaneous observation of effects of O₃ on both photosystems.

The objective of the present study was therefore to elucidate the effects of O₃ on photosystem functioning in intact leaf tissue by means of EPR

measurements of free radical intermediates in Photosystems I and II, and chlorophyll fluorescence transient kinetics. Since it is impossible to follow changes in EPR signals in excised leaf tissue over several hours because of the appearance of a large signal attributable to tissue wounding that appears after about one hour (Runeckles and Vaartnou, 1992), the studies were confined to intact, attached grass leaves.

Materials and methods

Plant material and growing condition

Kentucky bluegrass (*Poa pratensis* L.) plants were grown from seed in 5cm pots containing about 500 cc standard potting soil (85 loam; 15% peat) in a greenhouse. A slow release fertiliser 14:14:14 NPK (Osmocote; Sierra Chemical Company), was applied to the standard potting soil at planting at 0.5g/pot. About 50 seeds were sown per pot and these were thinned to 4 plants per pot, 5 days after sowing. The plantings were staggered in order to provide plants of the same age for the experiments. The plants were grown on the greenhouse bench at $25 \pm 3^{\circ}\text{C}$ and maximum illumination of $500 \mu\text{mol m}^{-2} \text{s}^{-1}$ (PAR) and exposed to O_3 at 6 weeks after sowing.

Exposure to ozone

The exposures were carried out within the quartz dewar insert in the cavity of the EPR spectrometer (Figure 1). Ozone levels approximated sine waves and were controlled by a program written for a 21X Micrologger (Campbell Scientific Inc.). Exposure commenced at 10:00h and the peak (120 ppb) occurred at 14:00h. To maintain a moist airflow over the leaf, compressed air from a cylinder of medical grade air was bubbled through distilled water. The flow rate was approximately 2 l min^{-1} through the quartz insert. Ozone was generated in the air stream by means of an ultraviolet source (Delzone Z0.300; Del Industries) and was monitored by sampling through a 3mm OD Teflon tube feeding to a Model 1003-AH O_3 monitor (Dasibi Environmental Corp).

Overall concentrations of O_3 were adjusted using needle valve/flow meter combinations to produce the desired maximum concentrations (120ppb). The selection of 120ppb maxima for both pollutants was based in part on the 1-hour average concentrations that are defined in the Federal Air Quality Objectives for Canada (82ppb), and the Air Quality Standards for the United States (120ppb).

Typical exposure regimes for O_3 and the control are given in Figure 2. The curves in Figure 2 were obtained with the distance weighted least squares

(DWLS) smoothing function of SYGRAPH (SYSTAT Inc.) and show the typical daytime rise in ambient O₃.

Illumination was supplied from a slide projector to the leaf through the slits in the cavity. Total white light intensity within the cavity was estimated to be 530 $\mu\text{mol m}^{-2}\text{s}^{-1}$ (PAR), obtained by halving the measured intensity at the surface of the cavity as per manufacturers's specifications. For far red light, obtained by using an optical bandpass filter (PTR Optics Ltd.), with 85% transmission at 710nm, the total intensity was estimated to be 10 $\mu\text{mol m}^{-2}\text{s}^{-1}$. The cavity was at room temperature (24 \pm 3⁰C).

Electron paramagnetic resonance (EPR)

EPR spectra were obtained using a Varian E-line X-band spectrometer (Varian). A model 5256A frequency converter (8-18GHz) (Hewlett.Packard) was used to measure frequency and a gaussmeter (Varian) to measure magnetic field strength. An E102 microwave bridge (Varian) generated microwaves. The microwave generator was connected to an E238 TM110 cavity (EPR cavity) via a 3 cm wide waveguide. An overview of the cavity and insert is shown in Figure 3.

The arrangement for positioning the end of an attached leaf within the quartz insert was described by Runeckles and Vaartnou (1992) and involved the loose attachment of the leaf to a T-shaped, cellulose acetate holder by means of cellulose adhesive tape with the lower leaf surface against the holder and the upper surface facing the cavity slits as shown in Figure 3. At each hour the following EPR signals were recorded: first the signal in white light, then the signal in 710nm light and lastly the signal in darkness. Between each spectrum a 2 min period was allowed for adaptation. Each spectral measurement took 4min. Spectra were recorded between 11:00 and 16:00h. The leaves were maintained in white light between measurements. For spectral recording the EPR conditions employed were:

Sweep width:	250G
Scan time:	4min
Time Constant:	0.128s
Power:	10mW
Detector current:	100 μ A
Gain:	5x10 ⁻⁴

Experimental design, spectra data handling, normalization and statistical analyses

In each experiment the two treatments were, control and O₃ exposure (n = 8). Typical first-derivative EPR spectra in Kentucky bluegrass are shown in Figure 4, illustrated the measurement of signal heights and showing *g*-values. In order to remove leaf-to-leaf variability the EPR signal height data were normalized to the value at 1100h (i.e. 1h after the start of the O₃ exposure wave). Additional experiments were conducted to examine the kinetics of Signal I changes resulting from changing light conditions. In these experiments, the leaves were mounted in the cavity at 10:00h and maintained in white light until the traces were recorded at 14:00h. Since the O₃ exposure wave started at 10:00h these traces were recorded at the time of the peak (120ppb). Traces like the one shown in Figure 5 were collected with the system locked onto the low-field maximum of Signal I and the leaf in darkness or illuminated with 710nm or white light in various sequences. Since the low field maximum of the first derivative of Signal I occurs at approximately the same field strength as that at which the first derivative of Signal II is close to zero, i.e. the maximum of the Signal II absorption spectrum, the effect of any changes in signal II on the amplitude of the first derivative of Signal I is minimal (Blumenfeld *et al.*, 1974). Each of the traces for a specific treatment (\pm O₃) were obtained using different leaves and hence were subject to leaf-to-leaf variability. As a result, between-treatment comparisons of signal heights in specific traces may not appear to show the same effects as those observed from the normalized means.

SYSTAT/SYGRAPH (Systat Inc.) was used for all statistical analyses and graphics. The DWLS (distance weighted least squares) function of SYGRAPH was used for curve-fitting to depict EPR and fluorescence data. Unless otherwise stated the trends depicted were established by polynomial contrasts.

Fluorescence measurements

A Portable Fluorometer (Model PAM2000; H.Walz GmbH, Effeltrich, Germany) with integrated Poquet PQ-1024 computer was used to measure fluorescence parameters. The parameters determined were derived from the measurement of Fo, Fm, Fm', Ft, defined as in Schreiber *et al.* (1994). The fluorescence parameters were measured on the first true leaf of one randomly selected plant from four pots for each treatment. At the end of dark adaptation, the following measurements were taken as follows: 1) Fo was measured using the measuring light (0.1 $\mu\text{mol m}^{-2} \text{s}^{-1}$), 2) a saturating pulse (12 000 $\mu\text{mol m}^{-2} \text{s}^{-1}$)

was applied to measure F_m , and 3) the saturating pulse was applied every 20s for the next 5min 20s, to measure F_t and F_m' . The full definition of the fluorescence parameters used in the present study is given in Table 1.

Table 1. Definition of chlorophyll nomenclature used in the present study

a. Fluorescence intensity indicators		
F_o	minimal fluorescence (dark)	fluorescence intensity with all PSII reaction centers open i.e, dark or low light adapted; $qP=1$ and $qN=0$.
F_m	maximal fluorescence (dark)	fluorescence intensity with all PSII reaction centers closed (i.e. $qP=0$) after dark or low light adaptation and all non-photochemical quenching processes at a minimum (i.e. $qN=0$).
F_v	variable fluorescence (dark)	maximum variable fluorescence with all non-photochemical processes are at a minimum; i.e. $F_m - F_o$.
F_t	fluorescence at any time	fluorescence intensity with a light-adapted sample
F_m'	maximal fluorescence (light)	fluorescence intensity with all Photosystem II (PSII) reaction centers closed in a light-adapted state; $qP=1$ and $qN \geq 0$.
b. Fluorescence quenching parameters		
qP	photochemical quenching	$(F_m' - F_t) / (F_m' - F_o)$
qN	non-photochemical quenching	$(F_m - F_m') / (F_m - F_o)$, the coefficient of non-photochemical quenching correlated with 'thylakoid membrane energization'.
NPQ	non-photochemical quenching	$(F_m - F_m') / F_m'$, the coefficient of non-photochemical quenching reflecting heat-dissipation of excitation energy in the antenna system
Y	Fluorescence quantum yield	$(F_m' - F_t) / F_m'$, the quantum yield of photochemical energy conversion reflecting the efficiency of the overall process.

Since the last six data points were found to represent a steady state in fluorescence, the means of the last four readings of Y , qP , and qN were used for data analysis. Photochemical quenching (qP), non-photochemical quenching correlated with 'thylakoid membrane energization' (qN), non-photochemical quenching (reflecting heat dissipation of excitation energy in the antenna system) (NPQ), and fluorescence quantum yield (Y) were calculated as given in Table 1. As it was not possible to modify the cavity itself, the threaded section at the top of the cavity was adapted to accommodate the fibre optic cable of the fluorometer (see Figures 1 and 3). A port for the illumination of the part of leaf viewed by the fibre-optic was provided to ensure that the same light intensity was used for both fluorescence and EPR measurements. These measurements

were taken at the same time as EPR measurements at hourly intervals from 11:00 to 16:00h. In order to remove leaf-to-leaf variability the fluorescence parameters were normalized to the value at 11:00h, as described for EPR spectral data above.

Results

Effects of O₃ on photosynthetic radicals

Ozone led to distinct increases in the relative height of the signals obtained in darkness (Signal II), white light (Signal I + II) and 710nm light (Signal I + II) (Figure 6). In the control the signals tended to decrease slightly with time. Two hours after the maximum O₃ concentration was reached (14:00h) the relative heights of the signals in white light and darkness were approximately 3 times the control. The signal in 710nm light behaved similarly but O₃ only resulted in a doubling of the relative height. It should be noted that the absolute signal heights in darkness were much less than in either white or far-red light. While the absolute heights of the white light signals were only about one half of the absolute heights of the 710nm light signals in the control, in O₃ their absolute heights were approximately equal and both were significantly greater than the 710nm light signals in the control.

The general relationship between signal heights in white and 710nm light is shown in the traces obtained in kinetic studies of Signal I observed at 14:00h illustrating the effects of switching among darkness (D) and illumination in white (W) or 710nm (F) light (Figure 7). As expected, the signal in 710nm light (F) was larger than the signal in white light (W) in the control. In the control, W caused a rapid increase in Signal I, which dropped back to a lower level within 10s, from which it tended to decline slowly. The “overshoot” of the signal at the start of W occurred after D. Ozone stimulated the signal in W so that the two signals were approximately equal (Figure 7). The saturation of the signal in W was slowed by O₃ (Figure 7) following a rapid initial rise to a level comparable to the control. Ozone caused a slower decay of the signal on switching from F to D relative to the control, after an initial rapid decline. In contrast, switching from W to D in O₃ resulted in a rapid decline to the baseline signal.

The O₃-induced slow decay of signal I in D after F was independent of the increased relative heights of signal II observed in D shown in Figure 7 since the latter were observed after 2min acclimation to darkness.

Effects of O₃ on chlorophyll fluorescence

In the control, there were slight but significant increased relative quantum yield (Y) and photochemical quenching (qP) over time to 13:00h, after which they remained virtually constant (Fig. 8 a and b). In O₃ neither Y nor qP changed over time, leading to significant decreases relative to the control. Both expressions of non-photochemical quenching (qN and NPQ) showed initial relative declines over time in the controls, while in O₃ they were constant (Figure 8 c and d, respectively). As a result, both qN and NPQ increased relative to the controls during the O₃ exposure period, with the maximum differences coinciding with the peak of O₃ exposure wave.

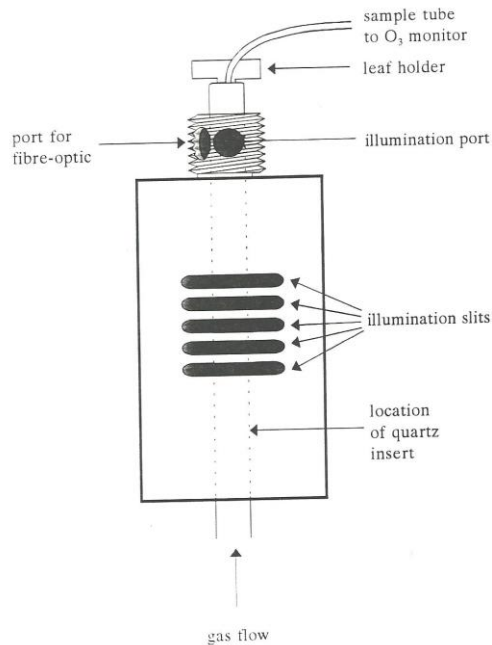


Fig. 1. The microwave cavity showing the adaptation of the threaded collar to accommodate the fibre-optic cable of from the fluorometer, and provide an additional illumination port.

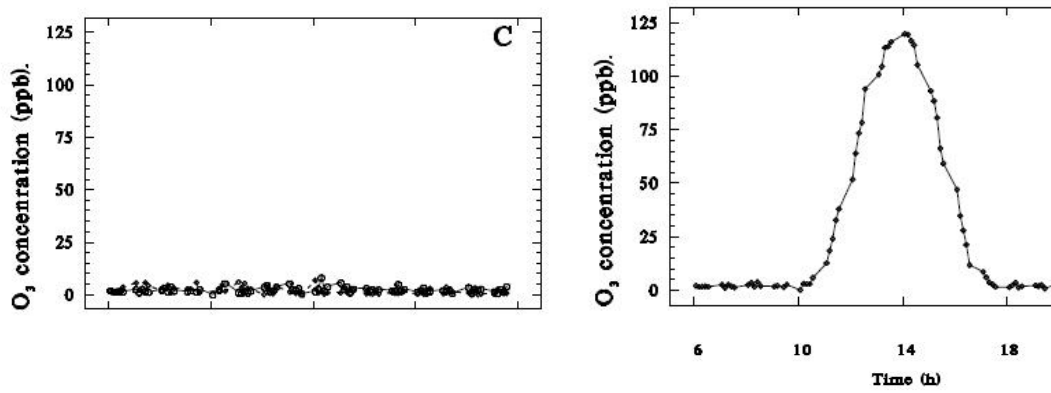


Fig. 2. The exposure regime for the O₃ (right) and ambient (left). The early O₃ was applied from 10:00 to 18:00h.

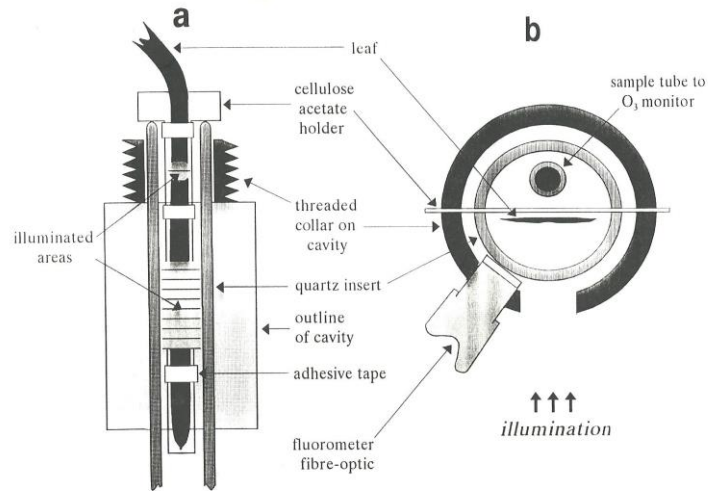


Fig. 3. Longitudinal (a) and cross-sectional (b) views of the cavity, showing the arrangement of leaf and leaf holder, the ozone sampling tube, the fluorometer fibre optic, and the illuminated areas of the leaf.

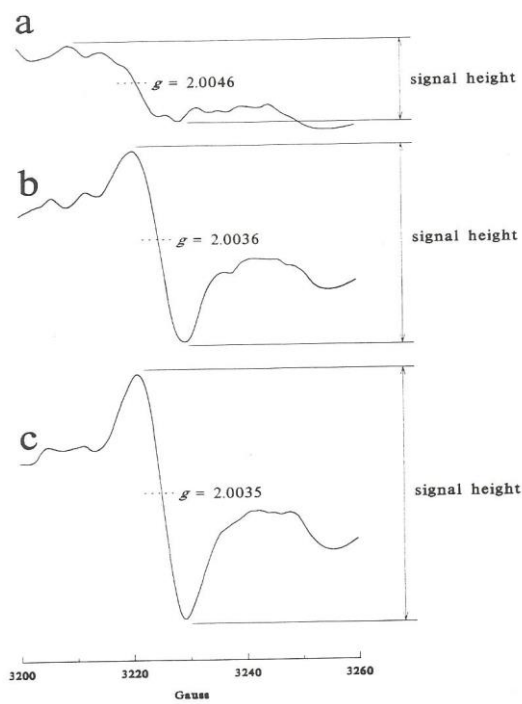


Fig. 4. Typical first derivative signals in a bluegrass leaf in a. Darkness; b. White light; c, 710nm light, illustrating height measurements and g-values (± 0.0002).

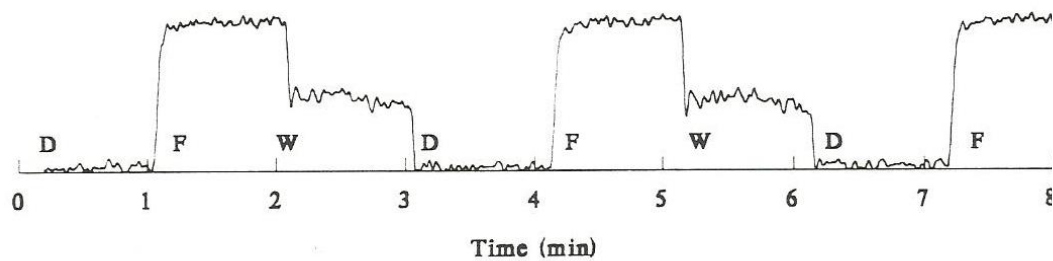


Fig. 5. Trace of Signal I low-field maximum in a bluegrass leaf in changing light conditions. D = darkness; F = 710 nm light; W = white light.

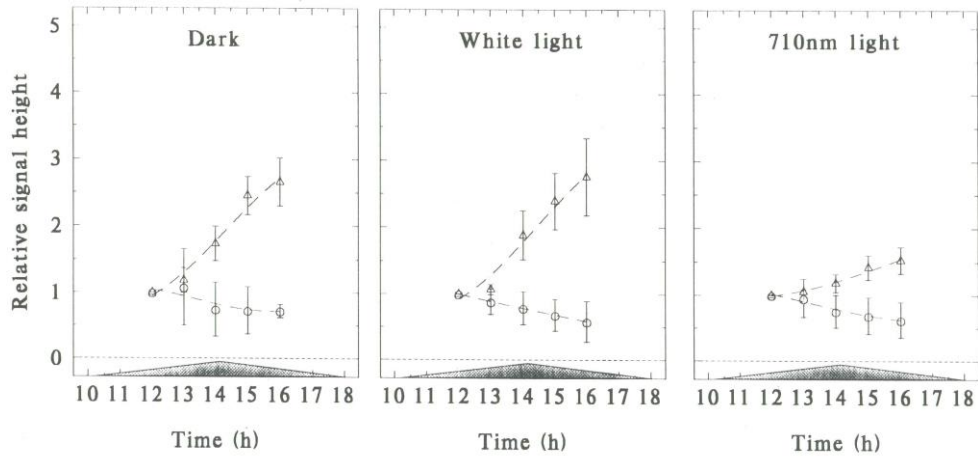


Fig. 6. Effects of O₃ on relative signal height in the dark, white or 710nm light for Kentucky bluegrass. Control (O); O₃ (Δ). Bars are SEDs based on individual means for each hour. N: 8.

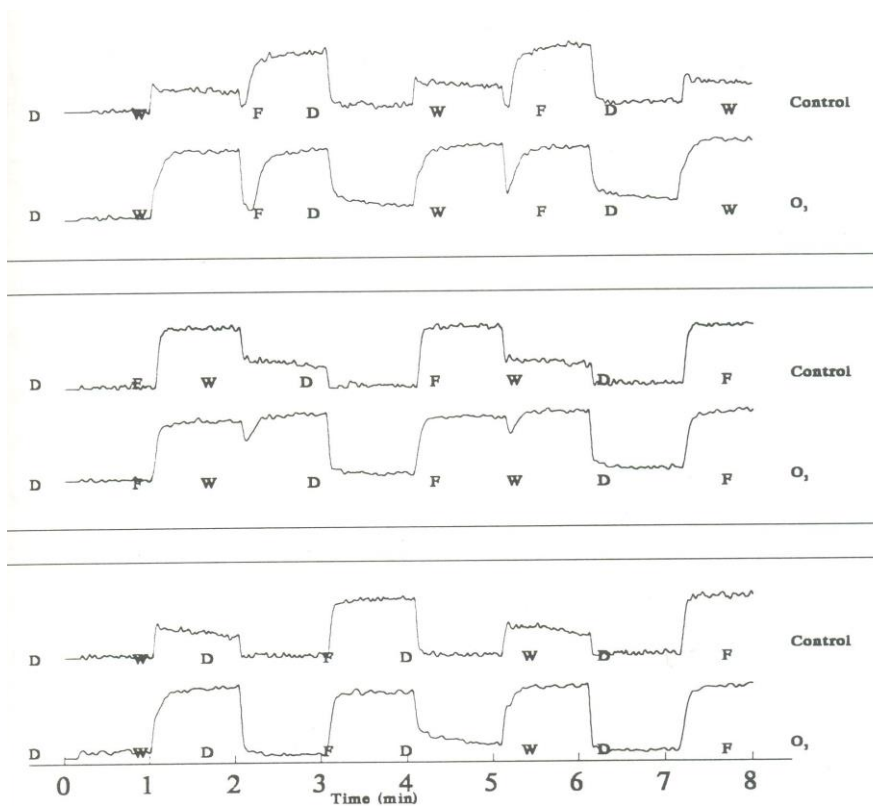


Fig. 7. Typical EPR Signal I traces for Kentucky bluegrass leaves in medical air or during exposure to 120 ppb O₃, with different sequences of illumination. D = dark; W = White light, F = 710 nm light.

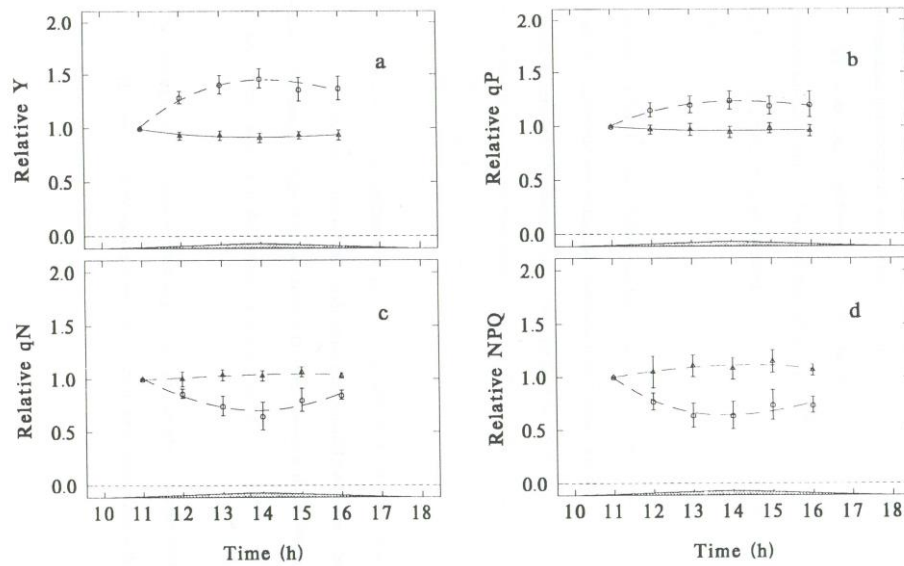


Fig. 8. Effects of O_3 on a. quantum yield (Y); b. photochemical quenching (qP); non-photochemical quenching (qN) and d, non-photochemical quenching (NPQ) in Kentucky blue grass. (O) control; (Δ) O_3 . Bars are SEDs, n=8.

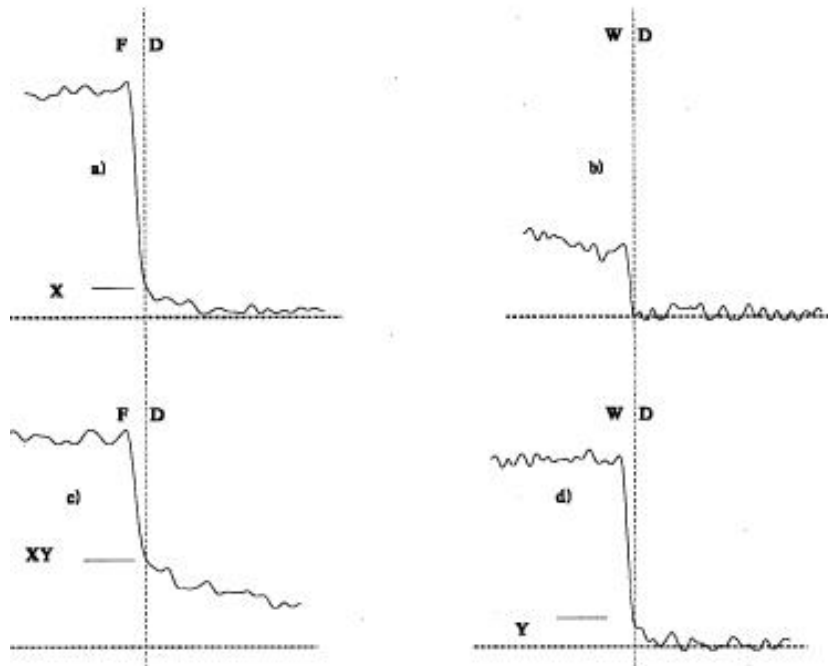


Fig. 9. Signal I decay kinetics: a. In 710 nm light in the control; b. In white light in the control; c. In 710 nm light during exposure to 120ppb O_3 ; and d. In white light during exposure to 120ppb O_3 . D = dark, W = white, F = 710nm light. X = limit imposed by reduced action of ferredoxin/NADP-reductase, and Y = limit imposed by inhibition of cyclic electron flow.

Discussion

Irradiation with far-red light typically leads to the appearance of a larger radical signal I, attributed to the oxidized P700 chlorophyll in photosystem I, than that observed in a mixture of red and far-red light or in white light as shown in Figure 4. This pattern of response is typical of radish (Runeckles and Vaartou, 1992) and many other C-3 species, including the blue-green alga, *Anacystis*, observed in an early study by Kok and Beinert (1962).

An “overshoot” followed by a decline was observed in Kentucky bluegrass at the start of exposure to white light (most noticeable after darkness). The overshoot and subsequent decline in Kentucky bluegrass are interpreted as being the result of the lag in the supply of electrons from photosystem II reaching the photosystem I centres permitting the amount of P700⁺ radical to rise initially above the equilibrium level.

EPR signals observed in intact leaves were inherently poorer in quality than those observed with chloroplast suspensions or algal cells, because of the increased heterogeneity of the tissue. Although there appear to have been no reports of tissue orientation dependence of EPR spectra of the photosynthetic radicals in leaves, such dependence has been demonstrated for the manganous ion which is largely concentrated in the chloroplasts. However, since with the grass species used in the present study the leaves were placed in the cavity with their blades perpendicular to the illumination, any possible contribution of orientation to an increase in heterogeneity must relate to the orientation of the chloroplasts within the mesophyll or bundle sheath cells or both.

Exposure to O₃ resulted in changes in both EPR signal characteristics and chlorophyll fluorescence parameters that indicated disturbance of the electron-flow between the photosystems. Thus O₃ suppressed the overshoot of Signal I observed at the start of illumination with white light in the control (Fig. 7) and the signal in white light continued to rise to the same level as that observed in 710nm light. This is typical of the situation observed in other systems in which the flow of electrons from PSII is blocked by the use of inhibitors such as 3(3,4-dichlorophenyl)-1,1-dimethylurea (DCMU) observed as early as 1962 by Kok and Beinert (1962). Close inspection of the rise of Signal I in white light observed in many traces revealed two components: a rapid rise to the level observed in the controls followed by a somewhat slower rise to the maximum (Fig. 7). In white light in O₃ the fast rise probably reflects the immediate formation of P700⁺, and the slower subsequent rise the establishment of a new equilibrium level determined by the reduced electron flow from PSII. The same mechanism could account for the slow maximizing of signal I in white light in foxtail in the presence of O₃ (Figure 7).

In Kentucky bluegrass, any inhibiting effect of O_3 on the flow of electrons to PSI cannot account for the slow decay of signal I during O_3 exposure observed at the end of illumination, particularly with 710 nm light (Fig. 7). Enlarged traces of these changes in air or O_3 are shown in Fig. 9. In darkness the decay in Signal I can only occur by transfers of electrons that are not light dependent, i.e. to NADP or to cytochrome b_6 (cyclic flow). Transfer to NADP is catalyzed by ferredoxin/NADP-oxidoreductase, which is light-induced. Inspection of the decay of Signal I on the transition from white to darkness in air shows an immediate drop to the baseline (Figure 9b). From 710nm light there is an immediate drop to a low level (X in Figure 9a) followed by a slow, reproducible decline to the baseline, suggesting that there was less oxidoreductase activity as a result of the lower overall light intensity (approximately one tenth of white light). As a result the final decay was rate-limited by the reduced oxidoreductase, while the rapid drop to X occurred by cyclic electron transfer to cytochrome b_6 and transfer to NADP although at a reduced rate. In the presence of O_3 , the final decay from white light was also retarded (from Y in Figure 9d) and a greater retardation was observed in the final decay from far-red light (from XY in Figure 9c). On the assumption that O_3 did not affect light-activation, the decline from white light could be accounted for by an O_3 inhibition of the oxidoreductase activity (from Y to the baseline) which becomes more pronounced in the drop from 710nm light because of the reduced activation of the enzyme (from XY to the baseline).

A summary of the changes in the different EPR signals and chlorophyll fluorescence parameters observed after the 6h exposure to O_3 wave which peaked at 120 ppb after 4h showed increases in Signal II observed in darkness, and the composites of Signals I and Signal II observed in both white and 710nm light over the controls, in both species.

The actual heights of the original dark signals were much less than those observed in white or far-red light. The heights of the actual signals in 710nm light in the controls were approximately double those in white light as indicated by the heights in the kinetic traces shown in Figure 4. Hence, Figure 6 indicates not only that the effects of O_3 on the white light signal were greater than those on the signal in 710nm light (as a result of reduced electron-flow from photosystem II discussed above) but that Signal I was also increased as a result of the prolonged exposure to O_3 .

The increased dark signal seen in Kentucky bluegrass is due to Signal II_s, which arises from Y_D^+ . Although Y_D does not appear to participate directly in oxygen evolution, it is thought to play a role in stabilizing and protecting the oxygen-evolving complex (Nugent *et al.*, 1987), perhaps by providing a supply of electrons as an alternative to the supply from Y_Z^+ , the normal donor to P680,

in the event of perturbation of the water splitting complex. Since the spectra of Signal II_s and Signal II_f have identical characteristics, the combined Signal II (slow +fast) in white light in the absence of O₃, would lead to an increase in the peak-to-peak height of the white light composite signals I and II by increasing the magnitude of the high field minimum, although the low field maximum would be little affected. This increase would be independent of any change in Signal I. However, since O₃ causes an increase in the dark signal attributable to Y_D⁺, this suggests that the normal flow of electrons from water-splitting through Y_Z⁺ to P680 has been impaired, and that the increase in the white light signal is the result of increases in both Signal II_s and Signal I. Of these changes only the enhancement of Signal I would be revealed by the traces of its low field maximum.

During a single exposure to O₃ the fluorescence quantum yield and photochemical quenching decreased over time relative to the control (Figure 8), which is in agreement with the fluorescence response observed in the presence of DCMU (Krause and Weis, 1991) or atrazine these together with the O₃-induced increases in non-photochemical quenching and the changes in EPR signals are compatible with the earlier suggestion that interference with water-splitting is a major consequence of exposure to O₃ (Schreiber *et al.*, 1978; Shimazaki, 1987).

In summary, the effects of O₃ were revealed by the observed changes in Signals I and II are indicative of reduced electron flow through PSI, and PSII. This suggests that the main effect of O₃ is on the electron acceptor side of PSII, and may involve impairment of the water-splitting process, as suggested by Schreiber *et al.* (1978) and others. The observed O₃-induced reduction in chlorophyll fluorescence quantum yield and photochemical quenching, and increase in both non-photochemical quenching parameters (qN and NPQ) are compatible with such an interpretation. Effects of O₃ on the kinetics of changes in Signal I on switching between different light exposures suggested that O₃ may also inhibit ferredoxin/NADP oxidoreductase.

References

- Asada, K. and Takahashi, M. (1987). Production and scavenging of active oxygen in photosynthesis. In "Photoinhibition", D.J. Kyle, C.B. Osmond & C.J. Arntzen, eds. Elsevier Science, Amsterdam. Pp. 227-287.
- Barry, B.A. and Babcock, G.T. (1987). Tyrosine radicals are involved in the photosynthetic oxygen-evolving system. Proc. Natl. Acad. Sci. USA 84:7099-7103.
- Blumenfeld, L.A., Goldfield, M.G., Tzapin, A.I. and Hangelov, S.V. (1974). Electron spin resonance signal I in leaves of higher plants: behaviour under simultaneous and separate illumination with red and far red light. Photosynthetica 8(3):168-175.

- Bussotti, F., Desotgiu, R., Cascio, C., Pollastrini, M., Gravano, E., Gerosa, G., Marzuoli, R., Nali, C., Lorenzini, G., Salvatori, E., Manes, F., Schaub, M. and Strasser, R.J. (2011). Ozone stress in woody plants assessed with chlorophyll a fluorescence. A critical reassessment of existing data. *Environmental and Experimental Botany* 73:19–30.
- Calatayud, A. (2007). Chlorophyll a fluorescence as indicator of atmospheric pollutant effects. *Toxicological & Environmental Chemistry* 89(4):627–639.
- Calatayud, A. and Barreno, E. (2004). Response to ozone in two lettuce varieties on chlorophyll a fluorescence, photosynthetic pigments and lipid peroxidation. *Plant Physiology and Biochemistry* 42(6):549–555.
- Calatayud, A., Iglesias, D.J., Talon, M. and Barreno, E. (2006). Effects of long-term ozone exposure on citrus: Chlorophyll a fluorescence and gas exchange. *Photosynthetica* 44 (4):548-554.
- Chanway, C.P. and Runeckles, V.C. (1984). Effect of ethylene diurea (EDU) on ozone tolerance and superoxide dismutase activity in bush bean. *Environ. Pollut. (Ser. A)* 35:49-56.
- Declaire, M., de Cat W., de Temmerman, L. and Baeten, H. (1984). Changes of peroxidase, catalase, and superoxide dismutase activities in ozone-fumigated spinach leaves. *J. Plant Physiol.* 116:147-152.
- Heath, R.L. (1988). Biochemical mechanisms of pollutant stress. In "Assessment of Crop Loss from Air Pollutants", W.W. Heck, O.C. Taylor & D.T. Tingey, eds. Elsevier Applied Science, London. Pp. 259-286.
- Kok, B. and Beinert, H. (1962). The light induced EPR signal of photocatalyst P700. II. Two light effects. *Biochem. Biophys. Res. Comm.* 9(4):349-354.
- Krause, G.H. and E. Weis (1991). Chlorophyll fluorescence and photosynthesis: The basics. *Ann. Rev. Plant. Physiol. Plant. Mol. Biol.* 42:313-349.
- Lee, E.H. and Bennett, J.H. (1982). Superoxide dismutase. A possible protective enzyme against ozone injury in snap beans (*Phaseolus vulgaris* L.). *Plant Physiol.* 69:1444-1449.
- Mudd, J.B. (1982). Effects of oxidants on metabolic function In "Effects of Gaseous Air Pollution on Agriculture and Horticulture", M.H.Unsworth & D.P.Ormrod, eds. Butterworth Scientific, London. Pp. 189-203.
- Nugent, J.H.A., Demetriou, C. and Lockett, C.J. (1987). Electron donation in photosystem II. *Biochim. Biophys. Acta* 894:534-542.
- Runeckles, V.C. and Chevone, B.I. (1992). Crop responses to ozone. In "Surface Level Ozone Exposures and Their Effects on Vegetation", A.S. Lefohn, ed. Lewis Publishers, Chelsea, MI. Pp. 185-266.
- Runeckles, V.C. and Vaartnou, M. (1992). Observations on the in situ detection of free radicals in leaves using electron paramagnetic resonance spectrometry. *Can. J. Bot.* 70:192-199.
- Sakaki, T., Kondo, N. and Sugahara, K. (1983). Breakdown of photosynthetic pigments and lipids in spinach leaves with ozone fumigation: role of active oxygens. *Physiol. Plant.* 59:28-34.
- Schreiber, U., Vidaver, W., Runeckles, V.C. and Rosen, P. (1978). Chlorophyll fluorescence assay for ozone injury in intact plants. *Plant Physiol.* 61:80-84.
- Shimazaki, K. (1988). Thylakoid membrane reactions to air pollutants. In "Air Pollution and Plant Metabolism", S. Schulte-Hostede, N.M. Darrall, L.W. Blank & A.R. Wellburn, eds. Elsevier, London. pp. 116-133.

(Received 10 September 2012; accepted 30 December 2012)